Respiration

Interventional Pulmonology

Respiration 2021;100:214–221
DOI: 10.1159/000512802

Received: June 7, 2020
Accepted: September 22, 2020
Published online: February 5, 2021

High Accuracy of Digital Tomosynthesis-Guided Bronchoscopic Biopsy Confirmed by Intraprocedural Computed Tomography

James Katsis[a] Lance Roller[a] Michael Lester[a] Joyce Johnson[b] Robert Lentz[a, c] Otis Rickman[a, c] Fabien Maldonado[a, c]

[a]Division of Allergy, Pulmonary and Critical Care Medicine, Vanderbilt University Medical Center, Nashville, TN, USA; [b]The Division of Pathology, Microbiology and Immunology, Vanderbilt University Medical Center, Nashville, TN, USA; [c]Department of Thoracic Surgery, Vanderbilt University Medical Center, Nashville, TN, USA

Keywords
Cone-beam computed tomography · Bronchoscopy · Lung nodule · Digital tomosynthesis · Electromagnetic navigational bronchoscopy

Abstract
Background: Digital fluoroscopic tomosynthesis-guided electromagnetic navigational bronchoscopy (F-ENB) is a novel adjunct to ENB associated with higher diagnostic yield. The likelihood of F-ENB allowing accurate placement of a biopsy needle within a target remains unclear. ***Objective:*** This study intends to determine the accuracy of F-ENB as confirmed by cone-beam computed tomography (CBCT) scan. ***Methods:*** Patients undergoing CBCT-assisted ENB for lung nodule biopsy were prospectively enrolled. ENB was performed followed by digital tomosynthesis correction. Once optimal F-ENB alignment was achieved, and a needle was advanced into the expected location of the nodule followed by CBCT. The primary outcome was the percentage of "needle-in-lesion" hits, defined as needle tip within the nodule in 3 planes. Secondary outcomes were diagnostic yield, procedure and room time, complications, radiation, and distance between the needle tip and nodule. ***Results:*** Twenty-six patients with a total of 29 nodules were enrolled. Mean nodule size was 13 mm (±4 mm) in maximal axial dimension, 83% ($n = 24$) were located in the peripheral third of the chest, and 17% ($n = 5$) had a bronchus sign. F-ENB guidance resulted in needle-in-lesion in 21 of 29 nodules (72%). Mean needle tip-to-nodule distance for nonhits was 1.75 mm (±1.35 mm). There were no complications. ***Conclusion:*** F-ENB resulted in a needle-in-lesion biopsy in greater than 70% of nodules despite features traditionally associated with poor diagnostic yield (size, absence of bronchus sign). Mean distance between needle tip and target for nonhits was less than 2 mm. These data suggest F-ENB alignment is accurate for small peripheral nodules.

Introduction

Lung nodules represent a significant clinical problem for patients and clinicians. They are common, often benign, but anxiety-provoking as they may represent the earliest stages of lung cancer. Two large randomized controlled trials have demonstrated significant reduction in lung cancer mortality with low-dose chest computed tomography (CT) screening of high-risk individuals [1, 2]. As screening increases, the identification of indetermi-

James Katsis
Interventional Pulmonology
Vanderbilt University Medical Center
1211 Medical Center Dr., Nashville, TN 37232 (USA)
jkatsis2@gmail.com

nate lung nodules is expected to rise, and with it the need for safe and effective biopsy techniques. The currently available minimally invasive biopsy modalities, CT-guided transthoracic needle biopsy (TTNB) and bronchoscopy, both have significant limitations. TTNB has traditionally been considered the gold standard due to the high diagnostic yield exceeding 90% in many studies [3]. However, complications are common with TTNB, including pneumothorax in 15–25% of cases and significant bleeding in 1–3% [3–5]. In addition, unlike bronchoscopy, TTNB does not allow for simultaneous biopsy of multiple nodules or mediastinal staging. Electromagnetic navigational bronchoscopy (ENB) is safer, with rates of pneumothorax approximately 3% and bleeding 1.5% but has been associated with disappointingly low diagnostic yield ranging from 40 to 70% [6–9].

Traditional ENB relies on pre-procedure CT scan to create a virtual tracheobronchial tree and a pathway to the target. However, the position of this virtual target, based on a CT scan at full inspiration in an awake spontaneously breathing patient, obtained weeks to months prior to the procedure, often differs from the actual position of the nodule in the anesthetized patient during bronchoscopy, a problem called CT-body divergence [10]. This has been frequently cited as a major limitation in the diagnostic yield of ENB [11].

Correction of traditional ENB using digital fluoroscopic tomosynthesis, or F-ENB, allows the bronchoscopist to make an intraprocedural correction for CT-body divergence. After navigation to the target nodule based on pre-procedure CT data, a conventional 2-dimensional (2D) C-arm fluoroscope is slowly swept through a 50-degree oblique arc while high-frequency fluoroscopic images are recorded. Digital tomosynthesis performed on the captured images provides a 3-dimensional reconstruction of the region of interest. The current location of the target nodule and catheter tip locations are marked by the proceduralist. This information updates the location of the target as projected on the navigation console, allowing the bronchoscopist to adjust and direct the catheter more precisely toward the nodule's current location. Aboudara et al. [12] recently demonstrated improved diagnostic yield of F-ENB compared to traditional ENB with no increase in complications. This technique may be particularly useful with smaller nodules and without a bronchus sign. However, it remains unclear if F-ENB alone is sufficient for optimal biopsy tool alignment or if it simply positions an expert operator close enough to optimize alignment using other tools such as radial probe endobronchial ultrasound (REBUS).

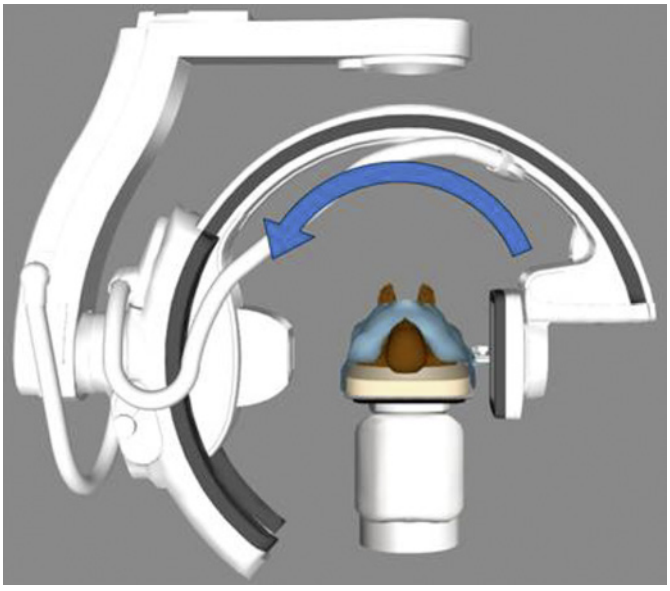

Color version available online

Fig. 1. Graphic demonstrating principles of CBCT. The X-ray beam source is located on the patient's left with a flat panel detector to the right. The 2 rotate opposite 1 another in a 180° spin around the patient, while 2D projection images are acquired. The data gathered from the spin are used for tomographic reconstruction of a high-resolution image volume that can be viewed in coronal, axial, and sagittal multi-planar reconstructions. (Image courtesy of Philips). CBCT, cone-beam computed tomography.

Cone-beam CT (CBCT) consists of an X-ray source which emits a cone-shaped beam opposite a flat panel detector. The images acquired are three-dimensional computer reconstructions of the data gathered during a 180° spin of the X-ray source and detector around the patient (Fig. 1).

The images allow the operator to confirm the biopsy instrument is within a nodule in axial, coronal, and sagittal planes ("needle-in-lesion"). There has been interest in CBCT bronchoscopy and its potential to improve bronchoscopic diagnostic yield [13, 14]. In this study, we sought to determine the accuracy of F-ENB as confirmed by intraoperative CBCT imaging.

Methods

Subjects

This was a prospective cohort study of consecutive patients referred for CBCT-assisted ENB at a single center. This study was approved by the Vanderbilt University Medical Center Institutional Review Board (Vanderbilt IRB #191443) as part of a quality improvement project collecting data on the impact of CBCT on bronchoscopy outcomes.

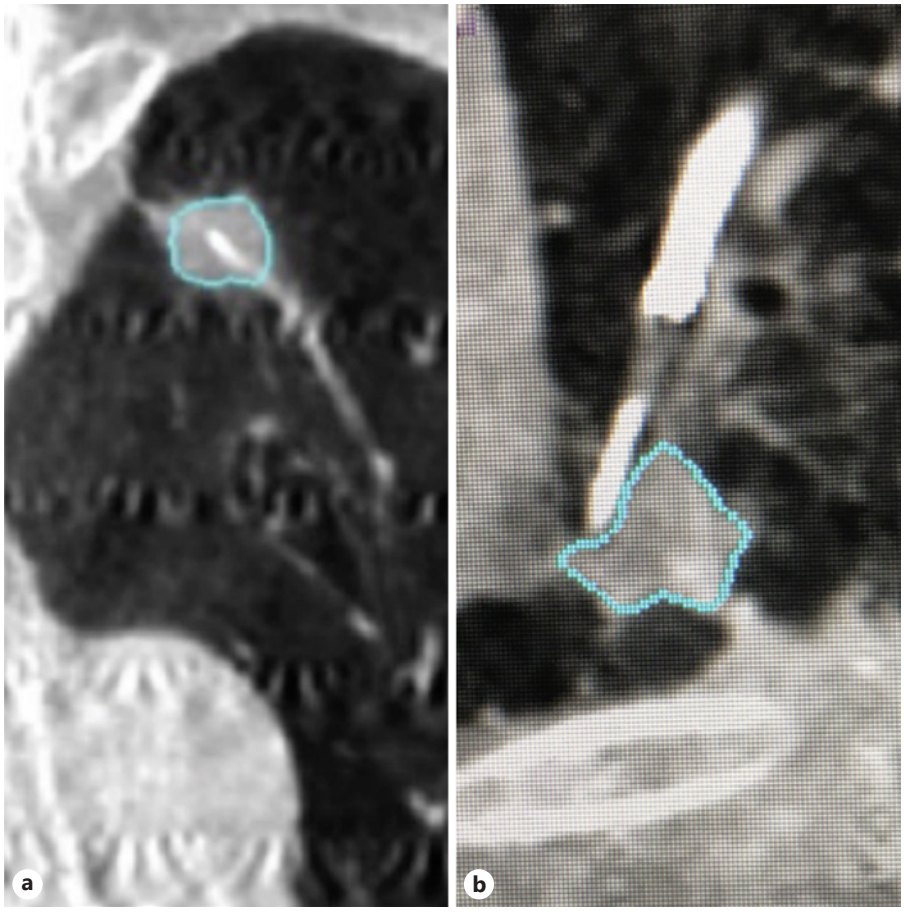

Color version available online

Fig. 2. a Image acquired from cone-beam computed tomography demonstrating needle-in-lesion in the coronal plane. Needle-in-lesion requires the needle to be in the operator defined nodule in 3 planes. **b** Coronal image demonstrating a miss.

Procedure

All procedures were performed in a hybrid operating room equipped with Philips Allura FD20 biplane system with Lung Suite Software (Phillips, Amsterdam, Netherlands), SuperDimension™ iLogic 7.2 ENB platform (SuperDimension™, Medtronic, Minneapolis, MN, USA), and a portable GE 9900 fluoroscopy C-arm (GE Healthcare, Chicago, IL, USA). A long sliding table allowed us to slide patients from under the C-arm to the biplane system with minimal interruption. All subjects received general anesthesia and neuromuscular blockade. A recruitment maneuver was performed immediately after intubation; fraction of inspired oxygen was minimized while maintaining SpO_2 above 90% to minimize absorption atelectasis, positive end-expiratory pressure was maintained at 15 cm H_2O, and lung-protective tidal volumes were used.

Technique

First, standard ENB was performed as previously described [12]. Following the initial navigation, a REBUS probe was inserted through the extended working channel (EWC). The locatable guide was reinserted and a 50° sweep was performed with the C-arm [12]. Using digital tomosynthesis, high-resolution images of the nodule are generated, and the true nodule location is marked. Alignment was then optimized based on the new target on the ENB platform, and REBUS was again used. A 21-gauge Arcpoint™ Pulmonary Needle (Medtronic, Minneapolis, MN, USA) was then advanced via the EWC into the expected location of the nodule. This process is explained in greater details in our original Aboudara et al. [12] publication. The C-arm was removed, and the bed was positioned under the Philips Allura system. A breath hold was initiated with positive end-expiratory pressure at 20 cm H_2O, and CBCT image acquisition using XperCT abd/thorax roll protocol was performed. The nodule was then segmented using Lungsuite© software. During segmentation, if the needle appeared to be within the nodule in all 3 planes, the biopsy was considered a successful "needle-in-lesion" hit (Fig. 2, 3).

During subsequent fluoroscopy, 3D roadmap© (Philips, Amsterdam, Netherlands) was utilized to generate an augmented fluoroscopy overlay of the nodule on live 2D fluoroscopic images. The operator was then allowed to adjust the EWC as desired to obtain diagnostic material, and REBUS visualization was repeated a final time.

Additional CBCT spins were performed as determined by the operator. Needle biopsy, forceps biopsy, and peripheral washing of the target were obtained at each site at operator discretion. If a patient had more than 1 nodule, the entire sequence above was repeated.

Histology Evaluation and Diagnostic Definitions

All biopsy specimens were evaluated by an expert lung pathologist. A specimen was considered diagnostic if any of the following

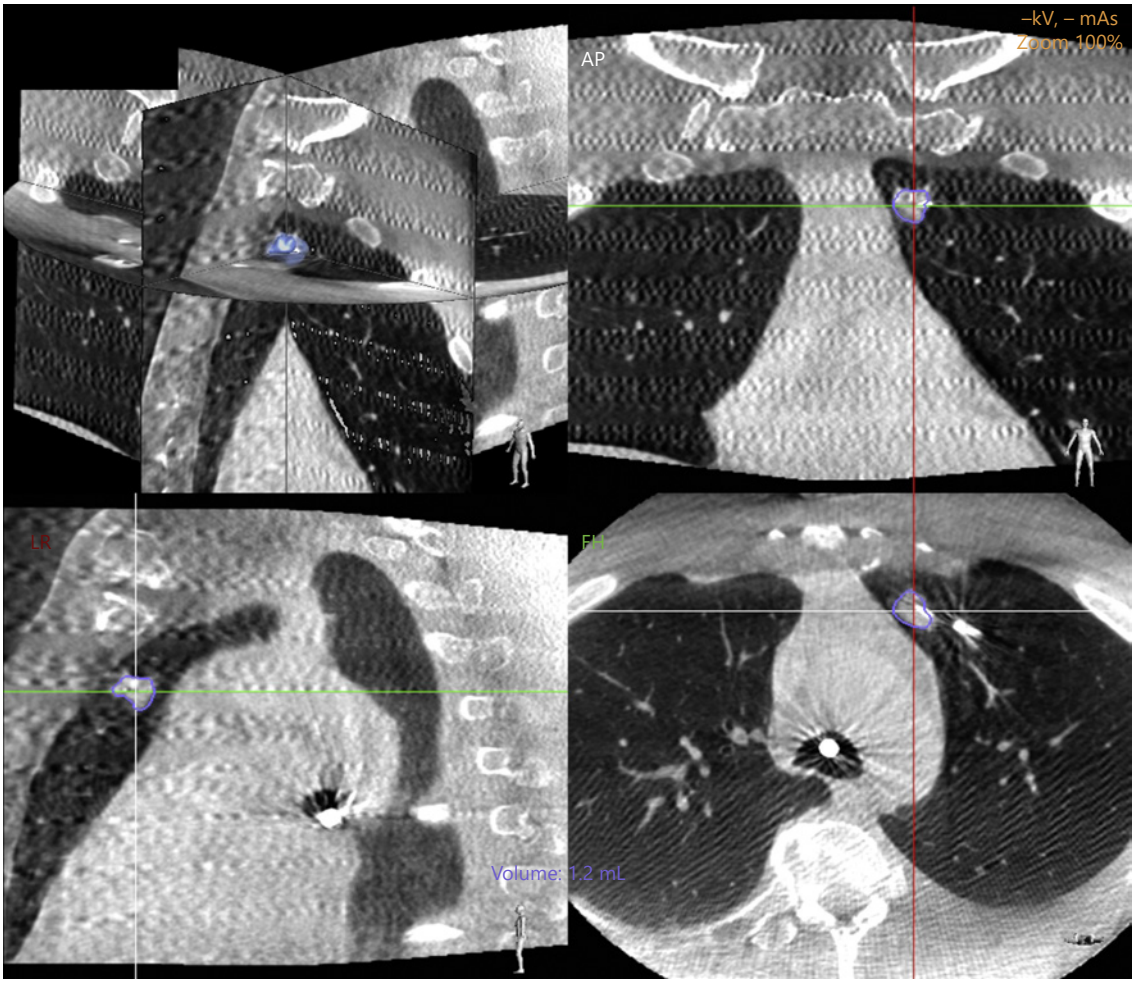

Color version available online

Fig. 3. Segmentation of a lung nodule using Lungsuite© software. The 3 planes here demonstrate an eccentric needle-in-lesion.

were met: (1) malignancy or (2) benign histological findings that could account for the presence of a nodule (e.g., granuloma). Normal lung parenchyma, nonspecific inflammation, "atypical," or "suspicious" cells not definitively malignant were considered nondiagnostic.

Outcomes

The primary outcome was percentage of first-pass needle-in-lesion biopsies achieved with needle placement guided by F-ENB (Fig. 3). Secondary outcomes included rates of diagnostic specimen acquisition, REBUS view (concentric vs. eccentric vs. no view of the nodule) at each iteration of the procedure (post-ENB, post-F-ENB, and post-CBCT), needle tip-to-nodule distance if the needle was not within the lesion in all 3 planes (tip to the closest nodule edge), procedure time, radiation dose, and rates of complications.

Statistical Analysis

Descriptive statistics including means with standard deviation for continuous variables and percentages and frequencies for categorical variables were reported. A multivariate logistic regression model using needle-in-lesion as our binary outcome was additionally utilized to identify variables associated with needle-in-lesion, using the following clinical variables: nodule size (mm), view on REBUS post-F-ENB (concentric, eccentric, and no view), and presence of a bronchus sign. The estimated odds ratios and 95% confidence intervals were provided to measure the effect of the association. Statistical analysis was performed using R version 3.6.1 (R Core Team [2019]).

Results

Between July 20, 2019, and March 21, 2020, 26 patients with a total of 29 nodules were enrolled. Mean age was 64 years (±12.4), and 65% were male. The median American Society of Anesthesiology overall health score was 3. Mean nodule maximal axial dimension was 13 mm (±4) with a mean volume of 1.25 mL (±1.5). Most nodules (83%) were

Table 1. Initial patient and nodule data

Patients, *n*	26
Nodules, *n*	29
Age	64 (SD: ±12.4, min: 31 max: 81)
Gender	
Male	17/26, 65%
Female	9/26, 35%
ASA median	3
Nodule size mean	12.8 mm (SD ±3.8 mL)
Nodules ≥2 cm	1 (3.4%)
Volume mean	1.25 mL (SD: ±1.54 mL)
Location, *n*	
RUL	9
RML	1
RLL	5
LUL	9
LLL	5
Peripheral 1/3rd of lung	24 (83%)
Middle 1/3rd	5 (17%)
Pleural to edge of nodule distance	1.2 cm (SD: ±1.4 cm)
Bronchus sign	5 (17%)

ASA, American Society of Anesthesiology.

Table 2. Pathologic results for each nodule

Malignant		
Adenocarcinoma	10	34.5%
Squamous cell carcinoma	9	31.0%
Lymphoma	1	3.4%
Benign lesional		
Organizing pneumonia	1	3.4%
Nondiagnostic		
Normal lung	3	10.3%
Neutrophils	1	3.4%
Chronic inflammation	1	3.4%
Atypical cells, nondiagnostic for malignancy	3	10.3%

within the peripheral third of the lung, with mean distance from nodule to pleural edge of 1.2 cm (±1.4). A bronchus sign was present in 5 of 29 (17%) nodules (Table 1).

Needle-in-lesion was observed in 21 of the 29 (72.4%) nodules. Histopathological diagnosis was confirmed in 21 of 29 nodules after readjustment of the biopsy instruments (72.4%, Table 2). Four specimens were diagnostic (13.7%) when F-ENB-guided needle was not initially within the lesion. Among the 8 first-pass biopsy attempts which were not needle-in-lesion, the mean distance from the needle to the closest edge of the nodule on axial cross sections was 1.75 mm ((±1.35 mm). In 13 of 29 nodules (44.8%), F-ENB improved REBUS view (nodule not visualized to eccentric view or eccentric view to concentric view) compared to standard ENB. In 8 of the 29 (28%) nodules, the REBUS view was improved with CBCT-based manipulations compared to F-ENB (Table 3). Despite a needle-in-lesion, we were unable to obtain histopathological diagnoses in 3 nodules.

The mean radiation dose per nodule was 259.6 mGy (±208.2 mGy), and the mean fluoroscopy time (including C-arm and CBCT) was 8.8 min (±5.3). The mean procedural time (measured from scope in to scope out) was 78.7 min (±28.1). This included mediastinal staging or additional diagnostic procedures in 15 of 24 (62.5%) patients. Mean in-room time was 118 min (±33). The multivariate analysis did not suggest nodule size, post-F-ENB REBUS signature, or bronchus sign were independent predictors of a needle-in-lesion. No complications occurred.

Discussion

In this single-center prospective case series, we report that F-ENB-guided transbronchial needle biopsy resulted in a needle-in-lesion in 72.4% of nodules, despite challenging nodule characteristics including small size (mean 13 mm diameter), peripheral location (mean distance from pleural edge of 1.2 cm), and a minority of nodules with bronchus sign (17%). The purpose of this study was to clarify the degree to which the digital tomosynthesis correction of nodule location using F-ENB achieved optimal biopsy alignment as confirmed by CBCT. F-ENB, when needle-in-lesion was not achieved, was still able to place the needle within 2 mm of the targeted nodule on average. Our data suggest that F-ENB is able to optimize alignment in the majority of cases even when nodules are small and peripheral. This supports the increased diagnostic yield noted by Aboudara and colleagues [12] after introduction of this technology in the only prior series describing F-ENB on diagnostic yield.

The secondary outcome of diagnostic yield does not strictly reflect the diagnostic yield of F-ENB, as more biopsies were obtained after CBCT-guided adjustments were made. Two prior reports describe CBCT-guided bronchoscopic diagnostic yield. Pritchett et al. [13] reported a diagnostic yield of 83.7% (77 of 92 nodules), while Casal et al. [15] reported a diagnostic yield of 70% (14 of 20 nodules). This was despite the former series targeting smaller nod-

Table 3. Rebus and CBCT views throughout the procedure

Nodule	REBUS view after ENB	REBUS view after F-ENB	REBUS view after cone beam	CBCT needle-in-lesion	Pathology
1	Concentric	Concentric	Concentric	Yes	Adenocarcinoma
2	Concentric	Concentric	Concentric	Yes	Adenocarcinoma
3	Eccentric	Concentric	Concentric	Yes	Normal lung
4	No view	Eccentric	Eccentric	No	Neutrophils
5	No view	No view	Eccentric	No	Normal lung
6	No view	No view	Eccentric	Yes	Normal lung
7	No view	No view	No view	No	Atypical cell, suspicious for malignancy
8	No view	Eccentric	Eccentric	Yes	Hodgkins lymphoma
9	Eccentric	Eccentric	Eccentric	Yes	Adenocarcinoma
10	No view	Eccentric	Concentric	Yes	Adenocarcinoma
11	No view	Eccentric	Eccentric	Yes	Squamous cell Ca
12	Eccentric	Eccentric	Eccentric	Yes	Squamous cell Ca
13	No view	Eccentric	Eccentric	Yes	Squamous cell Ca
14	No view	Eccentric	Concentric	Yes	Adenocarcinoma
15	Eccentric	Eccentric	Concentric	Yes	Atypical cell, suspicious for malignancy
16	No view	No view	Eccentric	No	Organizing Pneumonia
17	Eccentric	Eccentric	Eccentric	No	Adenocarcinoma
18	No view	Eccentric	Concentric	Yes	Adenocarcinoma
19	Concentric	Concentric	Concentric	Yes	Squamous cell Ca
20	Eccentric	Eccentric	Eccentric	Yes	Marked anthracotic pigment and chronic inflammation
21	No view	Eccentric	Eccentric	No	Squamous cell Ca
22	No view	Eccentric	Eccentric	Yes	Squamous cell Ca
23	Eccentric	Eccentric	Eccentric	Yes	Squamous cell Ca
24	Eccentric	Concentric	Concentric	Yes	Squamous cell Ca
25	No view	Eccentric	Concentric	Yes	Squamous cell Ca
26	No view	No view	Eccentric	No	Atypical squamous cells
27	No view	Eccentric	Eccentric	No	Adenocarcinoma
28	Eccentric	Eccentric	Eccentric	Yes	Adenocarcinoma
29	No view	No view	No view	Yes	Adenocarcinoma

CBCT, cone-beam computed tomography; ENB, electromagnetic navigational bronchoscopy; REBUS, radial probe endobronchial ultrasound.

ules (1.6 vs. 2.1 cm) and fewer with a bronchus sign (39 vs. 60%), variables previously suggested to be associated with diagnostic success [9, 16]. Pritchett and colleagues [11, 13] utilized ENB and EWC to access the nodule, similar to the current study, while Casal and colleagues [15] used thin or ultrathin bronchoscopy, which may have influenced yield. Casal and colleagues [15] also commented on atelectasis commonly obscuring targets in their series; different ventilation strategies, not well described by either series, might have also influenced these yields. Our diagnostic yield is similar to these prior studies; our nodules were smaller (1.3 cm), fewer demonstrated the bronchus sign (17%), and different definitions were used to define benign diagnostic histology, which may explain the reduction in diagnostic yield compared to Pritchett's series. Finally, these 2 prior studies, like this study, are all small single-center series of modest size and, therefore, may not be reflective of the true diagnostic yield for all peripheral nodules targeted bronchoscopically. Pritchett et al. [11, 13] recently evaluated the digital overlap of F-ENB and CBCT defined nodules. Digital overlap only needed to be >0% in order to be considered successful. 83% of (39/47) nodules had digital 3D target overlap after local registration. Radiologic confirmation of needle-in-lesion and digital target overlap is surrogates for the ultimate goal of diagnostic yield. Ultimately, the true yield of these technologies cannot be determined with small case series in single centers and comparative studies will be needed.

Interestingly, we were unable to obtain a pathological diagnosis in 4 of the CBCT documented first-pass needle-

in-lesion cases. This, in combination with the high degree of proximity to the target lesions, suggests that bronchoscopic yield may be limited by biopsy instruments used and pathological processing. The results we observed here are similar to our previously reported yield of 79% after the introduction of F-ENB [12]. The slight reduction in yield may be related to the smaller size of these lesions, lack of rapid on-site specimen evaluation during these cases and selection bias, as our team tended to select the most difficult cases for CBCT.

The mean radiation exposure for these procedures was 259 mGy, and the mean fluoroscopy time (including C-arm and CBCT) was 8.8 min. This is less than doses report with other common fluoroscopic procedures such as PCI [17]. Careful monitoring and mitigation of radiation exposure to both patients and providers should be optimized for centers considering CBCT-B.

This study has several limitations. It is single-center series from a group of expert bronchoscopists with significant experience with F-ENB, describing an experience with a modest number of targeted nodules. However, the maintenance of a high diagnostic yield despite inclusion of small nodules mostly without a bronchus sign remains a significant finding. There were significant limitations in the availability of the hybrid odds ratio which is why our numbers are small despite the enrollment period. Though specific pre-specified criteria were not utilized to determine which cases were selected for cone-beam guidance, the smaller nodule size and lower rate of bronchus sign in the current series compared to recent historical nodules targeted at this center [12] suggest more difficult targets were selected for cone-beam guidance, which argues against selection-based exaggeration of F-ENB targeting success or diagnostic yield. Additionally, we do not have follow-up data available to confirm our benign cases. However, the purpose of this study was to evaluate the accuracy of F-ENB itself. Adequate tissue acquisition depends on several other factors including sampling techniques and tissue characteristics. Pathological yield did not directly correlate to needle-in-lesion hit rate, likely due to issues with biopsy instruments, limitations in specimen evaluation, and readjustments made based on CBCT. Alternative biopsy techniques were discussed with all patients, including TTNB, which is also commonly performed for lesions of this nature. Navigational bronchoscopy, with rate of pneumothorax of 5% and significant parenchymal hemorrhage of 1% in a recent large series [8], has an overall lower complication rate than TTNB, while the diagnostic yield of TTNB for lesions under 1.5 cm has been reported to be 70% in a large case series [18], providing clinical rationale for the pursuit of such lesions via advanced bronchoscopy. TTNB admittedly remains the standard of case for a majority of nodules like those targeted in this series. Decisions to pursue TTNB or ENB will ultimately be guided by local expertise, availability of these new technologies, and patient preference.

In conclusion, F-ENB optimized instrument alignment to result in a needle-in-lesion in about 3 out of 4, further, demonstrating the potential for this ENB adjunct. A prospective multicenter trial is needed to confirm these preliminary findings.

Statement of Ethics

This study was approved by the Vanderbilt University Medical Center Institutional Review Board (Vanderbilt IRB #191443) as part of a quality improvement project collecting data on the impact of CBCT on bronchoscopy outcomes. Informed consent was waved.

Conflict of Interest Statement

Fabien Maldonado reports consulting fees and research support from Medtronic. Otis Rickman reports consulting fees from Medtronic. The other authors do not report any conflicts of interest.

Funding Sources

The authors did not receive any funding.

Author Contributions

James Katsis M.D. – Primary author. Collected data, built database, primary author of the manuscript, and primary study designer. Lance Roller M.S. – Secondary author and reviewer. Assisted with data collection, manuscript revisions, and edits and assisted with study design. Joyce Johnson M.D. – Secondary author, reviewer. Assisted with the manuscript revisions and edits. Reviewed pathological specimens. Michael Lester M.D. – Secondary author, reviewer. Assisted with data collection, study design, and manuscript revisions and edits. Robert Lentz M.D. – Secondary author, reviewer. Assisted with manuscript revisions, edits, study design, and data collection. Otis Rickman D.O. – Secondary author, reviewer. Assisted with manuscript revisions, edits, study design, and data collection. Fabien Maldonado M.D. – Secondary author. Primary reviewer and editor. Assisted with manuscript revisions and edits, study design, and data collection. All authors have provided final approval for publication.

References

1 Aberle DR, Adams AM, Berg CD, Black WC, Clapp JD, Fagerstrom RM, et al. Reduced lung-cancer mortality with low-dose computed tomographic screening. N Engl J Med. 2011;365(5):395–409.
2 de Koning HJ, van der Aalst CM, de Jong PA, Scholten ET, Nackaerts K, Heuvelmans MA, et al. Reduced lung-cancer mortality with volume CT screening in a randomized trial. N Engl J Med. 2020;382(6):503–13.
3 Dibardino DM, Yarmus LB, Semaan RW. Transthoracic needle biopsy of the lung. J Thorac Dis. 2015;7(Suppl 4):S304–16.
4 Wiener RS, Schwartz LM, Woloshin S, Welch HG. Population-based risk of complications following transthoracic needle lung biopsy of a pulmonary nodule. Ann Intern Med. 2011;155(3):137–44.
5 Heerink WJ, De Bock GH, De Jonge GJ, Groen HJM, Vliegenthart R, Oudkerk M. Complication rates of CT-guided transthoracic lung biopsy: meta-analysis. Eur Radiol. 2017;27(1):138–48.
6 Gex G, Pralong JA, Combescure C, Seijo L, Rochat T, Soccal PM. Diagnostic yield and safety of electromagnetic navigation bronchoscopy for lung nodules: a systematic review and meta-analysis. Respiration. 2014;87(2):165–76.
7 Wang Memoli JS, Nietert PJ, Silvestri GA. Meta-analysis of guided bronchoscopy for the evaluation of the pulmonary nodule. Chest. 2012;142(2):385–93.
8 Folch EE, Pritchett MA, Nead MA, Wolvers JJ, Khandhar SJ. Electromagnetic navigation bronchoscopy for peripheral pulmonary lesions: one-year results of the prospective, multicenter NAVIGATE study. J Thorac Oncol. 2019;14(3):445–58.
9 Ost DE, Ernst A, Lei X, Kovitz KL, Benzaquen S, Diaz-Mendoza J, et al. Diagnostic yield and complications of bronchoscopy for peripheral lung lesions: results of the AQuIRE registry. Am J Respir Crit Care Med. 2016;193(1):68–77.
10 Chen A, Pastis N, Furukawa B, Silvestri GA. The effect of respiratory motion on pulmonary nodule location during electromagnetic navigation bronchoscopy. Chest. 2015;147(5):1275–81.
11 Pritchett MA, Bhadra K, Calcutt M, Folch E. Virtual or reality: divergence between preprocedural computed tomography scans and lung anatomy during guided bronchoscopy. J Thorac Dis. 2020;12(4):1595–611.
12 Aboudara M, Roller L, Rickman O, Lentz RJ, Pannu J, Chen H, et al. Improved diagnostic yield for lung nodules with digital tomosynthesis-corrected navigational bronchoscopy: initial experience with a novel adjunct. Respirology. 2020;25(2):206–13.
13 Pritchett MA, Schampaert S, De Groot JAH, Schirmer CC, Van Der Bom I. Cone-beam CT with augmented fluoroscopy combined with electromagnetic navigation bronchoscopy for biopsy of pulmonary nodules. J Bronchology Interv Pulmonol. 2018;25(4):274–82.
14 Casal RF. Cone beam CT-guided bronchoscopy. J Bronchology Interv Pulmonol. 2018;25(4):255–6.
15 Casal RF, Sarkiss M, Jones AK, Stewart J, Tam A, Grosu HB, et al. Cone beam computed tomography-guided thin/ultrathin bronchoscopy for diagnosis of peripheral lung nodules: a prospective pilot study. J Thorac Dis. 2018;10(12):6950–9.
16 Ali MS, Sethi J, Taneja A, Musani A, Maldonado F. Computed tomography bronchus sign and the diagnostic yield of guided bronchoscopy for peripheral pulmonary lesions a systematic review and meta-analysis. Ann Am Thorac Soc. 2018;15(8):978–87.
17 Chon MK, Chun KJ, Lee DS, Lee SY, Hwang J, Lee SH, et al. Radiation reduction during percutaneous coronary intervention. Medicine. 2017;96(30):e7517.
18 Priola AM, Priola SM, Cataldi A, Errico L, Franco MD, Campisi P, et al. Accuracy of CT-guided transthoracic needle biopsy of lung lesions: factors affecting diagnostic yield. Radiol Med. 2007;112(8):1142–59.